ACS APPLIED MATERIALS & INTERFACES

Research Article

www.acsami.org

Electrochemical Analysis for Enhancing Interface Layer of Spinel $Li_4Ti_5O_{12}$: *p*-Toluenesulfonyl Isocyanate as Electrolyte Additive

Ren-Heng Wang, Xin-Hai Li,* Zhi-Xing Wang, Hua-Jun Guo, and Zhen-Jiang He

School of Metallurgy and Environment, Central South University, Changsha 410083, PR China

ABSTRACT: An electrolyte additive, *p*-toluenesulfonyl isocyanate (PTSI), is evaluated in our work to overcome the poor cycling performance of spinel lithium titanate ($Li_4Ti_5O_{12}$) lithium-ion batteries. We find that the cycling performance of a Li/$Li_4Ti_5O_{12}$ cell with 0.5 wt % PTSI after 400 cycles is obviously improved. Remarkably, we also find that a solid electrolyte interface (SEI) film is formed about 1.2 V, which has higher potential to generate a stable SEI film than do carbonate solvents in the voltage range of 3.0−0 V. The stable SEI film derived from PTSI can effectively suppress the decomposition of electrolyte, HF generation, interfacial reaction, and LiF formation upon cycling. These observations are explained in terms of PTSI including SO_3. The S═O groups can delocalize the nitrogen core, which acts as the weak base site to hinder the reactivity of PF_5. Hence, HF generation and LiF formation are suppressed.

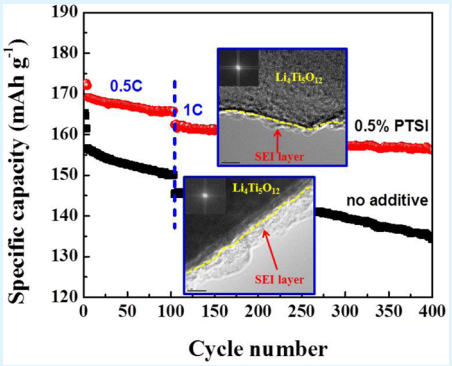

KEYWORDS: *lithium-ion battery, spinel lithium titanate, elevated temperature property, nonaqueous electrolyte, electrolyte additive, solid electrolyte interphase layer, p-toluenesulfonyl isocyanate*

1. INTRODUCTION

Spinel lithium titanate ($Li_4Ti_5O_{12}$) possesses a relatively high and flat lithium insertion/extraction voltage at about 1.55 V (vs Li^+/Li) compared to the commonly used anode materials, whereas the operating voltage of graphitic anodes is only about 0.25 V. Thus, the generation of solid electrolyte interface (SEI) layers and the electroplating of lithium can be averted.[1−4] Moreover, $Li_4Ti_5O_{12}$ exhibits outstanding Li^+ ion mobility and reversibility in the cycled process.[5−8] Therefore, it can be concluded that $Li_4Ti_5O_{12}$ can offer an excellent safety advantage over graphitic anodes, which may be applied to large-scale and long-life energy-storage devices as a potential anode material.[1,9]

Unfortunately, $Li_4Ti_5O_{12}$ has a lower intrinsic lithium-ion diffusion coefficient (ca. 10^{-19} to 10^{-16} cm^2 s^{-1}) and electronic conductivity (ca. 10^{-13} S cm^{-1}) because Ti 3d exhibits a band-gap energy in the range of 2.0−3.0 eV and can result in poor high-rate charge/discharge capabilities.[10,11] Moreover, $Li_4Ti_5O_{12}$-based batteries will swell in the charge/discharge and storage processes, which is likely ascribed to the generated gases (e.g., CO, CO_2, and H_2) reacting from $Li_4Ti_5O_{12}$ and the surrounding alkyl carbonate solvents interface.[12] In view of electrolyte, the performance deterioration of Li/$Li_4Ti_5O_{12}$ cell is mainly attributed to the generated acidic impurity HF from $LiPF_6$ salt decomposition in the presence of trace water, especially at elevated temperatures, which is believed to accelerate electrolyte decomposition. Various methods for improving the Li/$Li_4Ti_5O_{12}$ cell electrochemical performance have been proposed, such as improving the electron transfer between the current collector and the active material,[13] preparation of nanoparticles,[14,15] doping with cations,[14,16] and forming composites with carbon and metal powder,[17,18] among others. Therefore, researchers mainly have focused on the synthesis and characterization of $Li_4Ti_5O_{12}$. Electrolyte additives are an effective and economic method to enhance Li-ion battery performance.[19] Electrolyte additives can not only decrease electrolyte oxidation at the cathode but also hinder transition metal dissolution and modify SEI film to reduce LiF formation on the anode surface. It is reported that a SEI film is generated over 1.0 V because of the reaction of electrolyte/$Li_4Ti_5O_{12}$ electrode interface, greatly enhancing the cycling and high-rate performance of the electrode.[20]

p-Toluenesulfonyl isocyanate (PTSI) possesses good physical properties, as shown in Table 1. In addition, the energies of the lowest unoccupied molecular orbital (LUMO) (−0.2469 Ha) and highest occupied molecular orbital (HOMO) (−0.0935 Ha) of PTSI are both lower than those of vinylene carbonate (VC, LUMO = −0.2274 Ha, HOMO = −0.0412 Ha).[21,22] That is to say, PTSI can readily accept electrons and has a high oxidation potential.

Table 1. Physical Properties of PTSI (25 °C)

ρ (g cm^{-3})	μ (Pa s^{-1})	T_f (°C)	T_b (°C)	T_m (°C)	σ (mS cm^{-1})
1.295	2.72	145	270	5	7.95

On the basis of the above advantages, PTSI is chosen as an electrolyte additive. The focus of our work is to study the interface between the electrolyte and $Li_4Ti_5O_{12}$ electrode to reveal mechanism for SEI film formation. In addition, because diethyl carbonate (DEC)-based electrolyte decomposition

Received: August 1, 2015
Accepted: October 9, 2015
Published: October 9, 2015

DOI: 10.1021/acsami.5b07047
ACS Appl. Mater. Interfaces 2015, 7, 23605−23614

reactions resulting from attacked PF_5 produce HF, we especially use DEC as one of the solvents to better reveal the SEI film formation mechanism between $Li_4Ti_5O_{12}$ and carbonate ester electrolyte interface. PTSI includes SO_3, and the −S═O groups can delocalize the nitrogen core, which acts as the weak base site to hinder the reactivity of PF_5. We expect that the stable SEI film of $Li_4Ti_5O_{12}$ electrode is able to effectively suppress HF generation and LiF formation to enhance the cyclic performance of the $Li_4Ti_5O_{12}$ electrode.

2. EXPERIMENTAL SECTION

2.1. Preparation of the Electrolyte. A base electrolyte (Jiangxi Youli New Materials Co., Ltd., China) was a 1 M $LiPF_6$ in ethylene carbonate (EC)/ethyl methyl carbonate (EMC)/DEC (1:1:1, wt %). The desired amount (0.5 wt %) of PTSI additive was dissolved in the base electrolyte and stirred 5 min in an argon-filled glovebox, and the oxygen and water content were less than 1 ppm. The supernatant was measured using a Karl Fischer 831 Coulometer (Metrohm) for H_2O and Karl Fischer 798 GPT Titrino (Metrohm) for HF, respectively. The contents of H_2O and HF in the electrolyte were restricted to under 10 ppm.

2.2. Electrochemical Characterization. $Li_4Ti_5O_{12}$ electrodes were prepared by coating a slurry of 80 wt % $Li_4Ti_5O_{12}$ (Sichuan Xingneng Co., Ltd., China), 10 wt % acetylene black (AB), and 10 wt % poly(vinylidene fluoride) (PVDF) and then blended in *N*-methyl-pyrrolidinone (NMP). The mixture slurry was spread uniformly on a thin copper foil and dried under vacuum for 12 h at 120 °C. The 14 mm diameter electrode disks were then punched out of the coated foil sheets. Li/$Li_4Ti_5O_{12}$ were assembled for 2025-type coin cells in the argon-filled glovebox with Celgard 2400 as separator.

Linear sweep voltammetry (LSV) and cyclic voltammetry (CV) data were generated by an instrumental electrochemical workstation (CHI604E, Chenhua, Shanghai) with a three-electrode system incorporating $Li_4Ti_5O_{12}$ as the working electrode and lithium foils as both counter and reference electrodes at a scan rate of 0.1 mV s^{-1}. Electrochemical impedance spectroscopies (EIS) of Li/$Li_4Ti_5O_{12}$ cells after 3 cycles and 100 cycles between 3.0 and 1.0 V were recorded under discharge to 1.0 V, and the open-circuit voltages (OCVs) of the cells were used as the initial potential. A sinusoidal amplitude modulation was used over the frequency range of 0.01 Hz to 100 kHz, and the perturbation amplitude was 5 mV.

2.3. Surface Analyses of the Electrode. $Li_4Ti_5O_{12}$ electrodes were rinsed with DMC three times and dried in a vacuum drier at 45 °C for 4 h. The phase structure was measured by X-ray diffraction (XRD, Rint-2000, Rigaku) using Cu Kα radiation in an angular range of 10−90° (2θ) with a 0.02° (2θ) step. Microstructure and morphology of $Li_4Ti_5O_{12}$ electrodes were visualized. Microstructure of the $Li_4Ti_5O_{12}$ electrode were recorded using scanning electron microscopy (SEM, JEOL, JSM-5600LV, Japan) with an accelerating voltage of 20 kV. Transmission electron microscopy (TEM, Tecnai G12, 200 kV) characterized the surface morphology of $Li_4Ti_5O_{12}$ electrodes. The chemical components of $Li_4Ti_5O_{12}$ electrodes surface were analyzed by X-ray photoelectron spectroscopy (XPS, K-Alpha 1063, Thermol Fisher).

3. RESULTS AND DISCUSSION

3.1. Cycling and Rate Performance Analyses. Figure 1a shows the cyclic performance of Li/$Li_4Ti_5O_{12}$ cells at room temperature (25 °C) in a voltage range of 3.0−1.0 V (vs Li/Li^+). It can be observed that cells with PTSI have better cycling performance than those with no additive. The first capacity of a cell with no additive is 147.7 mAh g^{-1} at 1 C. However, the first capacities of the cells with electrolyte containing 0.3, 0.5, and 1.0 wt % PTSI are 152.6, 166.6, and 161.7 mAh g^{-1}, respectively. After 65 cycles, the capacity of cell with no additive is 143.4 mAh g^{-1}, and the capacities of the cells with electrolyte containing 0.3, 0.5, and 1.0 wt % PTSI are 149.1, 164.2, and 159.2 mAh g^{-1}, respectively. It is suggested that the incorporation of PTSI can

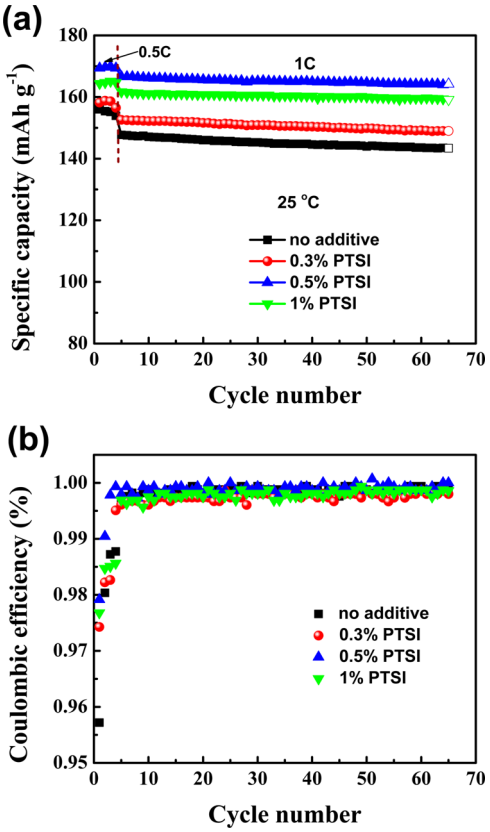

Figure 1. (a) Cycling performances. (b) Coulombic efficiency of Li/$Li_4Ti_5O_{12}$ cell with different electrolytes cycled between 3.0 and 1.0 V at 25 °C.

significantly improve the capacity stability, and the cell with electrolyte containing 0.5 wt % PTSI has superior cycling performance compared to that with other concentrations of PTSI added. Coulombic efficiencies of cells are shown in Figure 1b. The Coulombic efficiencies of PTSI-containing Li/$Li_4Ti_5O_{12}$ cells are better than that of the cell with no additive, particularly the initial efficiency. As a result, the electrolyte with 0.5% PTSI is chosen to study in the paper.

The cycling performances of a $Li_4Ti_5O_{12}$ electrode discharged to 1.0 V at charge/discharge rates of 0.5 and 1 C are shown in Figure 2a. Compared with the Li/$Li_4Ti_5O_{12}$ cell with no additive, the Li/$Li_4Ti_5O_{12}$ cell with 0.5 wt % PTSI exhibits excellent cycle performance during 400 cycles. The capacity retention of Li/$Li_4Ti_5O_{12}$ cell with no additive after 400 cycles is only 81.4%, which is much lower than that of Li/$Li_4Ti_5O_{12}$ cell with 0.5 wt % PTSI (90.7%), as shown in Table 2. Thus, the Li/$Li_4Ti_5O_{12}$ cell with PTSI shows much better cyclic stability. It may be ascribed that PTSI can restrain the reduction decomposition of electrolyte and decrease the consumption of electrolyte.

To confirm that the introduction of PTSI into the electrolyte facilitates faster kinetics of the $Li_4Ti_5O_{12}$ electrode, a rate performance study is carried out. Figure 2b,c show the rate performance of the Li/$Li_4Ti_5O_{12}$ cells with and without PTSI-containing electrolyte. It can be seen that the cell with 0.5 wt % PTSI displays better rate performance than that with no-additive electrolyte, suggesting that the incorporation of PTSI can enhance the kinetics of $Li_4Ti_5O_{12}$ electrode.

To further understand the electrochemical performance of $Li_4Ti_5O_{12}$ electrode, the first charge/discharge profiles at different discharge current densities from 0.1 to 5 C at 55 °C

DOI: 10.1021/acsami.5b07047
ACS Appl. Mater. Interfaces 2015, 7, 23605−23614

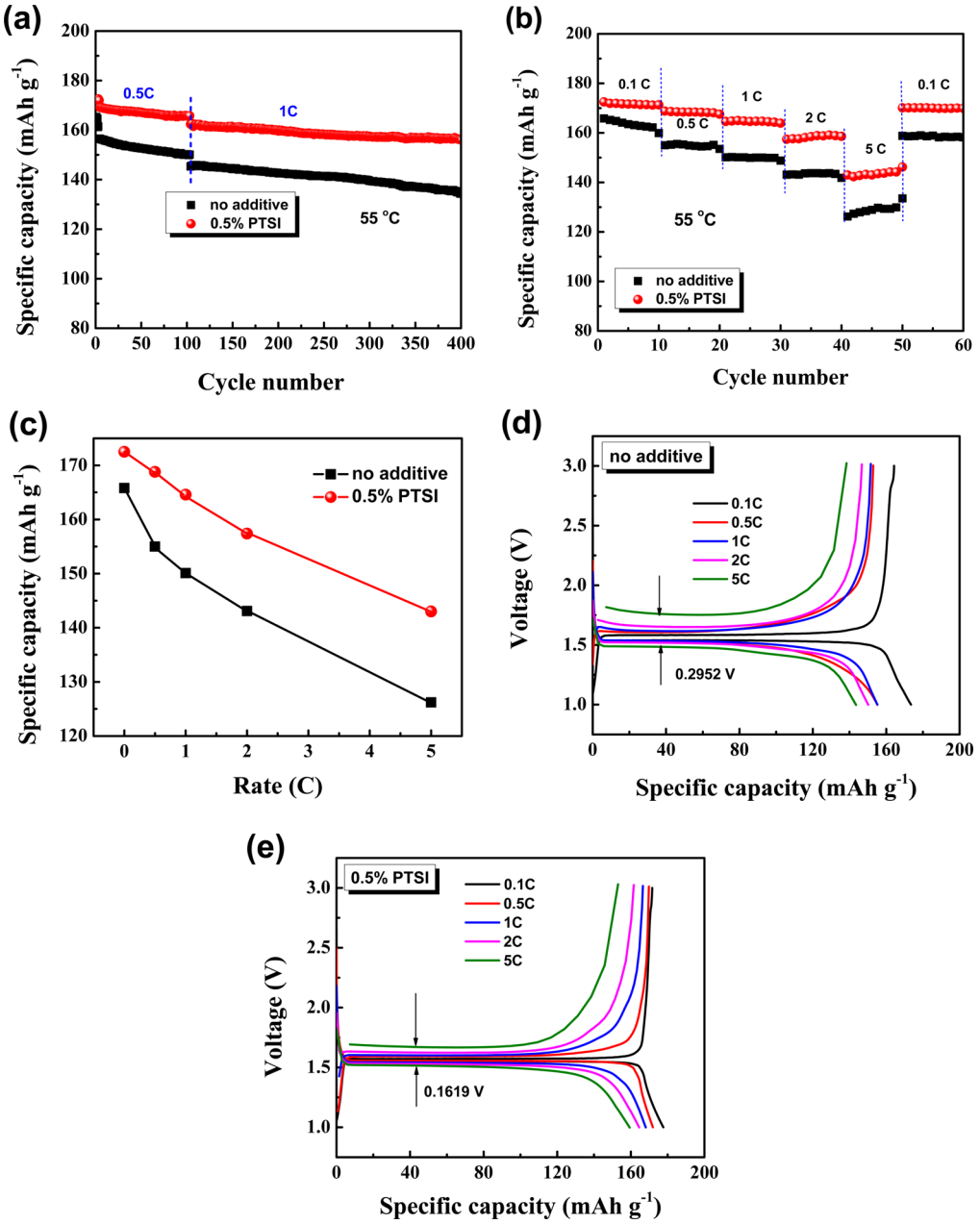

Figure 2. (a) Cycling performance of Li/$Li_4Ti_5O_{12}$ cell with and without PTSI additive. (b and c) Rate performance and (d and e) charge/discharge curves of Li/$Li_4Ti_5O_{12}$ cell with and without PTSI additive cycled between 3.0 and 1.0 V at different current rates from 0.1 to 5 C at 55 °C.

Table 2. Capacity Retention of Li/$Li_4Ti_5O_{12}$ Cell with Different Electrolytes

	no additive		0.5% PTSI	
	specific capacity (mAh g^{-1})	retention (%)	specific capacity (mAh g^{-1})	retention (%)
50th	152.5	92.2	166.9	97.1
100th	150.1	90.8	165.7	96.3
400th	134.6	81.4	156.2	90.7

are shown in Figure 2d,e. The specific discharge capacities of the cell with no additive carried out at 0.1, 0.5, 1, 2, and 5 C are 164.3, 152.9, 151.6, 146.7, and 138.3 mAh g^{-1}, respectively. The capacity at 5 C is 84.2% of the value at 0.1 C. For the cell with 0.5 wt % PTSI, the specific discharge capacities are 171.7, 169.8, 166.6, 161.6, and 159.4 mAh g^{-1}, respectively. It can be seen that the specific discharge capacities of the cell with 0.5 wt % PTSI is also excellent, especially at large current densities. The capacity at 5 C is 92.8% of the value at 0.1 C. This indicates that the rate discharge performance of Li/$Li_4Ti_5O_{12}$ cell with 0.5 wt % PTSI is greatly improved. As is well-known, the thin SEI film can be helpful to shorten the lithium-ion diffusion channel and improve electronic conductivity. It is suggested that the layer on the Li/$Li_4Ti_5O_{12}$ cell with PTSI-containing electrolyte is thinner than that of the Li/$Li_4Ti_5O_{12}$ cell with no additive, and the Li/$Li_4Ti_5O_{12}$ cell with PTSI-containing electrolyte shows better rate charge and discharge performance.

Moreover, it is interesting to note from Figure 2d,e that the two electrodes show much different cycling performance at different current densities applied. The electrode with 0.5 wt % PTSI possesses more stable initial cycling performance at 0.1 C than that without additive and contrariwise for longer cycles at a

DOI: 10.1021/acsami.5b07047
ACS Appl. Mater. Interfaces 2015, 7, 23605−23614

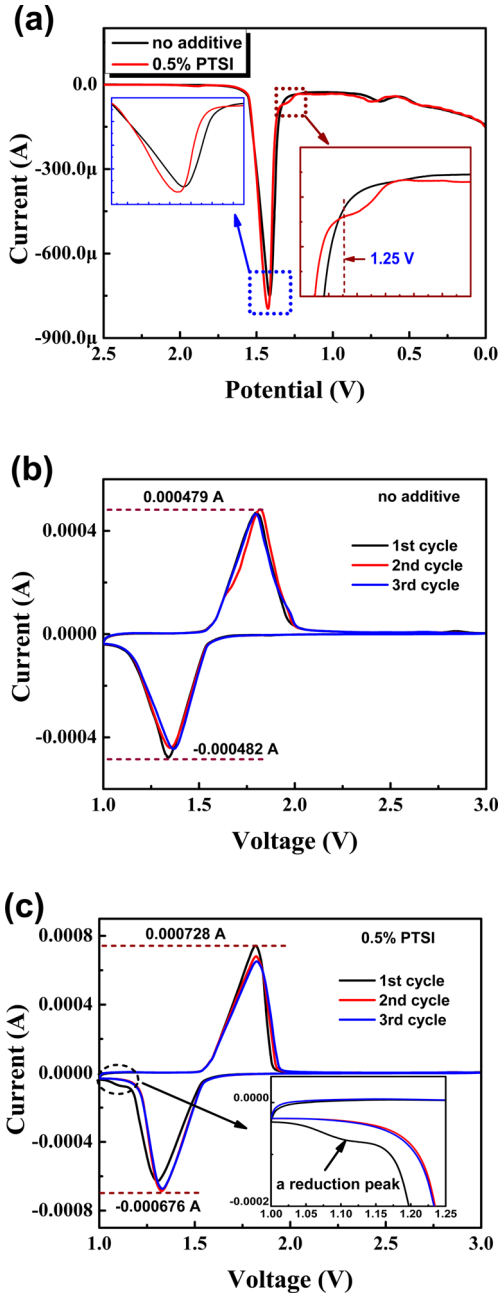

Figure 3. (a) LSV and (b and c) CV of Li/$Li_4Ti_5O_{12}$ cell with no additive and 0.5 wt % PTSI, respectively, at a scan rate 0.1 mV s^{-1}.

larger current. In addition, the lithiation/delithiation potential of the cell with 0.5 wt % PTSI is 0.1619 V at 5 C, which is smaller than that of the cell with no additive (0.2952 V), indicated by its higher voltage difference Li^+ intercalation/deintercalation. The smaller polarization of the PTSI-containing electrolyte supports the fact that the $Li_4Ti_5O_{12}$ has better kinetics, which is thought to reduce activation barriers for facile Li^+ migration.

3.2. LSV and CV Measurements of Li/$Li_4Ti_5O_{12}$ Cells with Different Electrolytes. To investigate the potential range of the additive, we controlled the potential of a working electrode against Li in a LSV experiment. Figure 3a displays LSV curves of a Li/$Li_4Ti_5O_{12}$ cell without and with PTSI. It can be seen that there is one reduction peak at 1.46 V because of the lithium-ion insertion from the $Li_4Ti_5O_{12}$ structure, whereas the peak potential of PTSI-containing electrode is a little higher than that of the no-PTSI electrode. Moreover, because of a consequence of unsignificant lithiation polarization, the peak current of PTSI-containing electrode is normally stronger than that of no-PTSI electrode. In addition, for the electrolyte with 0.5 wt % PTSI, a little reduction peak appears at ~1.25 V. This peak is originated from $Li_4Ti_5O_{12}$/electrolyte solution interfacial reactions,[21] which is the formation of SEI film on $Li_4Ti_5O_{12}$ surface. Therefore, PTSI has higher potential to form a SEI film than do carbonate solvents.

The CV curves are shown in Figure 3b,c. Both Li/$Li_4Ti_5O_{12}$ cells have two sharp, symmetrical redox peaks around at 1.46 and 1.67 V, which is in agreement with the lithium-ion intercalation/deintercalation of the spinel structure. The peak currents of the Li/$Li_4Ti_5O_{12}$ cell with 0.5 wt % PTSI is obviously larger than those of the cell with no additive. This result is consistent with that of Figure 2c,d. Part of the loss capacity is used to generate the original SEI film, leading to a large irreversible capacity, which in turn restrained further interfacial reactivity and reduced the peak current. In contrast, the interfacial reaction of the $Li_4Ti_5O_{12}$ electrode with 0.5 wt % PTSI is much lower; hence, the capacity is mainly due to lithiation of the electrode, resulting in stable CV curves and original cycling performance. As a result, the Li/$Li_4Ti_5O_{12}$ cell with 0.5 wt % PTSI possesses better rate performance. In addition, there is a reduction peak at ~1.18 V for the PTSI-containing electrolyte, which is agreement with LSV measurements.

3.3. Impedance Analysis. EIS of Li/$Li_4Ti_5O_{12}$ cell without and with PTSI were recorded to characterize the surface properties of electrode, as shown in Figure 4. The two spectra exhibit different characteristics at high and medium frequencies. According to the previous reports of impedance of lithium-ion batteries, the semicircle at high frequency (interfacial layer resistance, R_f) is relevant to the impedance of Li^+ migration from the electrolyte to the electrode, and the semicircle at medium frequency (charge transfer resistance, R_{ct}) can be related to the impedance of charge transfer of the electrode and the Warburg impedance (W_0), which is ascribed to solid-phase diffusion of Li ion in the bulk of the intercalation compound.[23−25] Nyquist diagrams were fitted on the basis of the equivalent circuits as the insets of Figure 4a,b. The fitting results are listed in Figure 4c. It is interesting that the cell with PTSI has R_f and R_{ct} lower than those of the cell with no additive. The surface layer resistance is 27.3 and 7.6 Ω for the cell without and with PTSI after three cycles at room temperature, respectively. However, the surface layer resistance grew significantly for the cell with no additive after 100 cycles, from 27.3 to 214.9 Ω, whereas the growth of impedance is negligible for the cell with PTSI (from 7.6 to 119.3 Ω). It is expected that the addition of PTSI favors the formation of SEI in good condition, which both the Li^+ migration through the surface film of $Li_4Ti_5O_{12}$ and the transfer of charge in electrochemical reaction can be prompted by the decomposition products of PTSI. Therefore, compared to the cell with no additive, the two semicircles with PTSI are significantly decreased. The change in the corresponding process of SEI film formation is shown in Figure 4d. The lowered impedances of surface layer and charge transfer of the electrode decrease ohmic polarization and activation polarization during repeated lithiation/delithiation, confirming the previously mentioned superior rate capacity.[26]

3.4. SEM, XRD, and TEM Analyses. To make certain the source of the performance of the Li/$Li_4Ti_5O_{12}$ cell with PTSI, SEM micrographs of the $Li_4Ti_5O_{12}$ electrodes are shown in Figure 5a−c. The micrographs of the electrodes cycled without and with PTSI reveal a very different topography. Compared to

DOI: 10.1021/acsami.5b07047
ACS Appl. Mater. Interfaces 2015, 7, 23605−23614

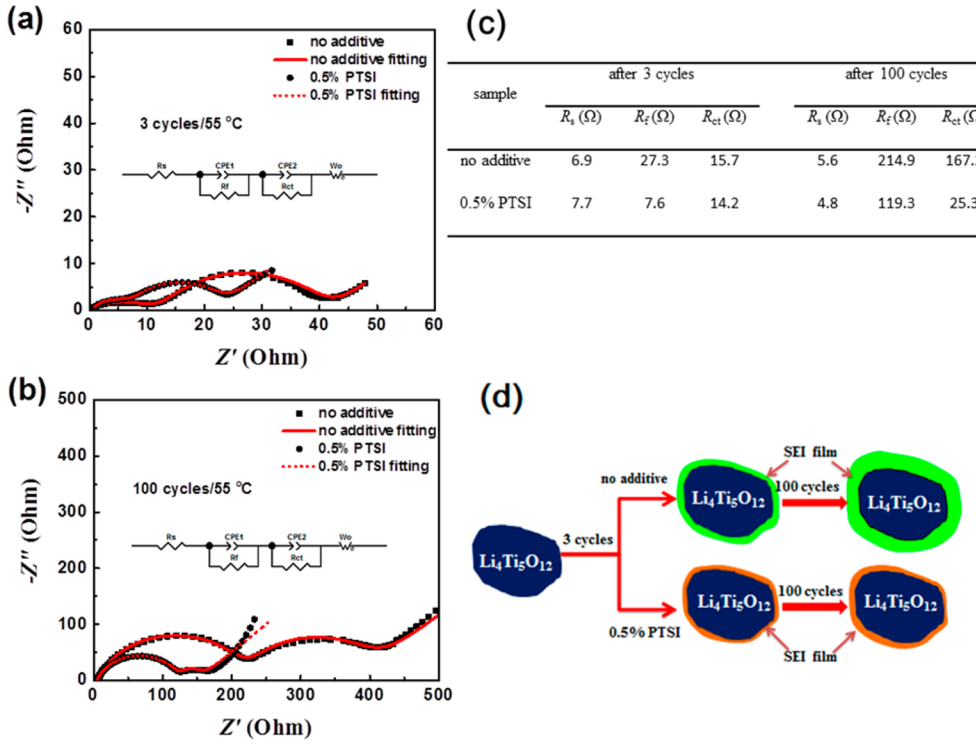

sample	after 3 cycles			after 100 cycles		
	R_s (Ω)	R_f (Ω)	R_{ct} (Ω)	R_s (Ω)	R_f (Ω)	R_{ct} (Ω)
no additive	6.9	27.3	15.7	5.6	214.9	167.2
0.5% PTSI	7.7	7.6	14.2	4.8	119.3	25.3

Figure 4. Impedance spectra of discharged Li/$Li_4Ti_5O_{12}$ cell with and without 0.5 wt % PTSI additive at 55 °C: (a) after 3 cycles of 0.1 C charge−discharge (b) after 100 cycles of 0.5 C charge−discharge. (c) EIS fitting results of two samples and (d) the process illustration of SEI film formation.

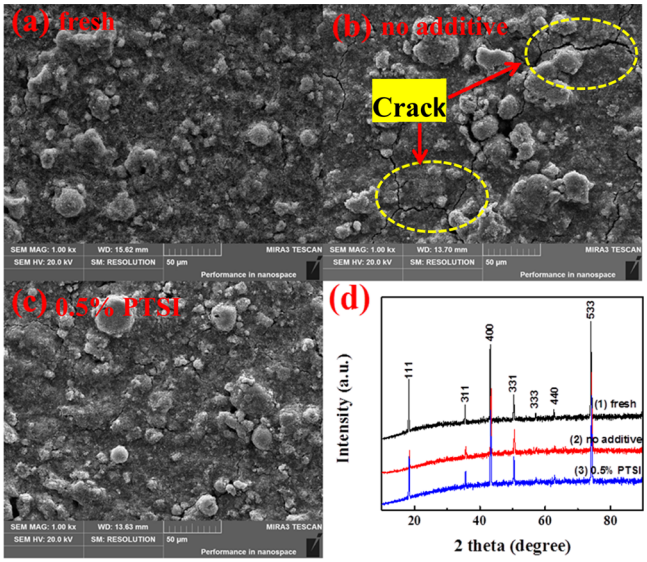

Figure 5. SEM images of $Li_4Ti_5O_{12}$ electrodes: (a) fresh, (b) no additive, and (c) with 0.5 wt % PTSI after 100 cycles at 55 °C. (d) XRD of $Li_4Ti_5O_{12}$ electrodes.

the fresh electrode (Figure 5a), the morphology of the $Li_4Ti_5O_{12}$ electrode with no additive displays an obvious change (Figure 5b). There are some cracks among particles on the electrode. However, the particles on the $Li_4Ti_5O_{12}$ electrode with PTSI (Figure 5c) are less crushed than those with no additive, which is attributed to the cathode/electrolyte interface film.[27] PTSI possesses relatively small viscosity, which can improve the electrolyte seepage properties of electrode materials. Meanwhile, PTSI has higher potential than carbonate solvents during the voltage range of 3.0−0 V. HF formation is hindered, and the $Li_4Ti_5O_{12}$ electrode is not corroded by HF. To clarify the effect of

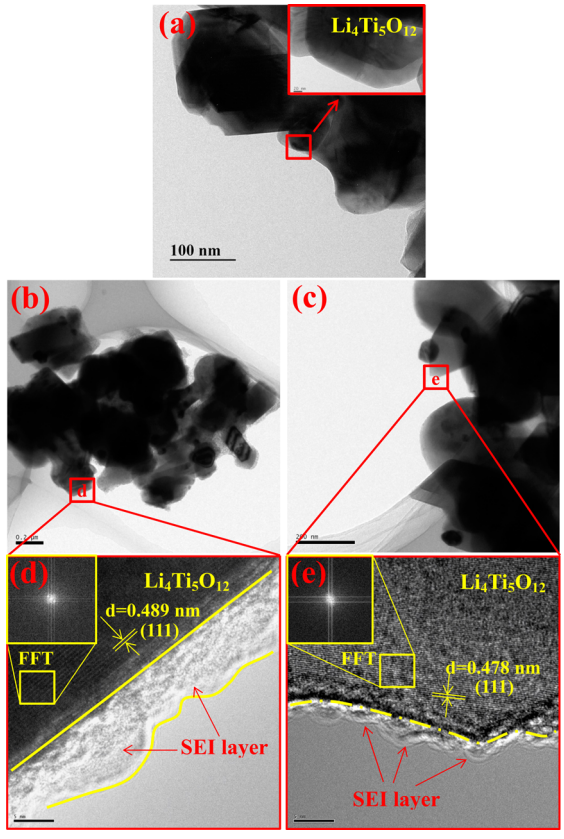

Figure 6. TEM images of $Li_4Ti_5O_{12}$ electrodes: (a) fresh, (b and d) no additive after 100 cycles at 55 °C, and (c and e) with 0.5 wt % PTSI after 100 cycles at 55 °C.

DOI: 10.1021/acsami.5b07047
ACS Appl. Mater. Interfaces 2015, 7, 23605−23614

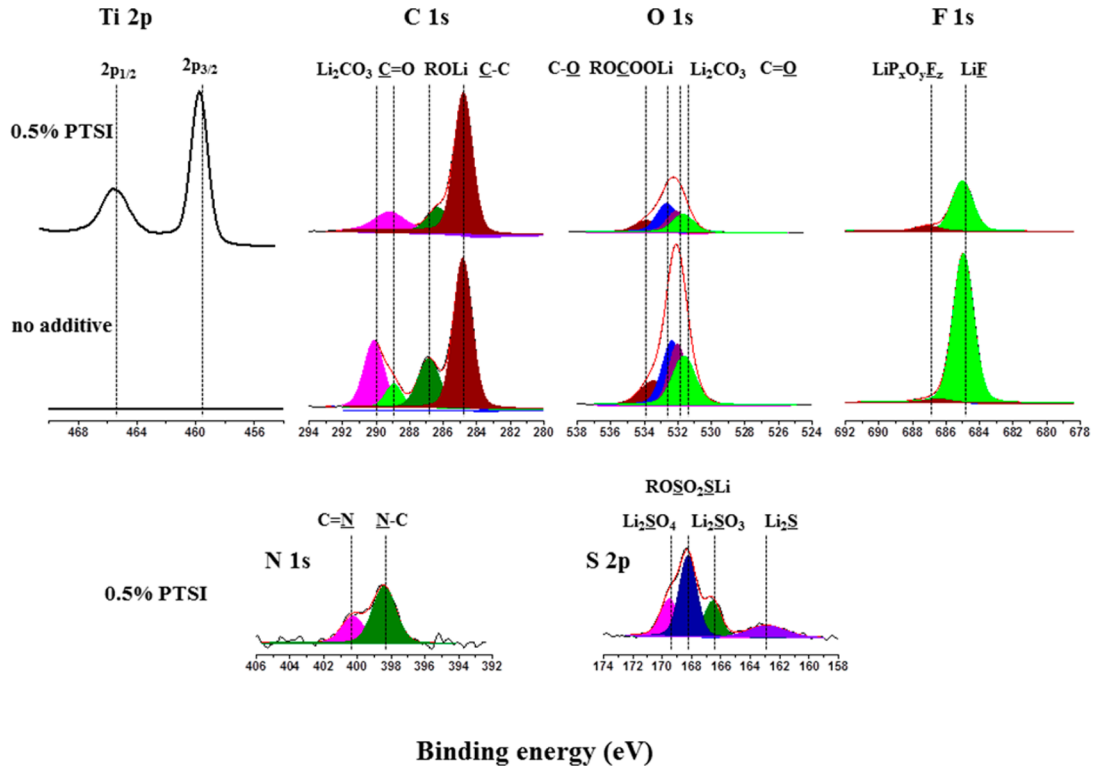

Figure 7. XPS survey spectra of $Li_4Ti_5O_{12}$ electrode after 100 cycles at 55 °C without and with additive.

Scheme 1. Autocatalytic Thermal Decomposition of $LiPF_6$-Based Carbonate Electrolyte

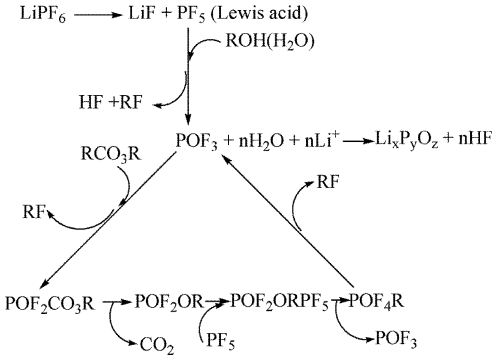

the structures of two samples, the phase structure was characterized using power XRD; a diffraction pattern is revealed in Figure 5d. All peaks can be indexed as $Li_4Ti_5O_{12}$ (space group *Fd*3*m*, PDF No. 49-0207, International Centre for Diffraction Data, 2003).[28,29] No other peaks such as TiO_2 were found. That is to say, the structure of $Li_4Ti_5O_{12}$ is not affected by the additive.

Furthermore, to clarify the effect of PTSI on the $Li_4Ti_5O_{12}$ electrode at 55 °C, surface analysis of the cycled electrodes was obtained. Figure 6 shows TEM micrographs of a fresh $Li_4Ti_5O_{12}$ electrode and the cycled $Li_4Ti_5O_{12}$ electrodes with different electrolytes. The surface of fresh electrode is flat and smooth, as shown in Figure 6a. However, a clear boundary can be detected on the $Li_4Ti_5O_{12}$ electrode after 100 cycles in Figure 6d,e. The surfaces of the electrodes are covered with a layer, which is known to be SEI film. It is seen that there is a thicker layer on the electrode surface with no additive.

In contrast, the layer generated from the PTSI-containing electrolyte displays a uniformly thinner film on the $Li_4Ti_5O_{12}$ electrode surface. According to impedance analysis, this thinner layer can reduce the interfacial resistance of $Li/Li_4Ti_5O_{12}$ and improve Li^+ migration rate via the surface layer of $Li_4Ti_5O_{12}$ and the transfer of charge in electrochemical reaction. The result indicates that PTSI-containing electrolyte can suppress to a certain extent the decomposition reactions of solvent, which is consistent with the rate performance described above. The high-resolution TEM (HRTEM) images and the fast Fourier transform (FFT) patterns further indicate that there is a well-defined crystal structure of two samples. The *d* spacings of 0.489 nm of the without-additive electrode and 0.478 nm of the $Li_4Ti_5O_{12}$ electrode with PTSI particles match well with that of the (111) plane of $Li_4Ti_5O_{12}$. Although the *d* spacing parameters of the $Li_4Ti_5O_{12}$ electrode with/without PTSI additive differ from each other, it is mostly ascribed to the intrinsic reactivity between $Li_4Ti_5O_{12}$ and alkyl carbonate solvents. The $Li_4Ti_5O_{12}$ electrode initiates the decomposition reactions of EC and DEC subjected to charge/discharge cycles.[12] In addition, the $Li_4Ti_5O_{12}$ electrode is corroded by HF. The SEI film on $Li_4Ti_5O_{12}$ electrode with PTSI can hinder $Li_4Ti_5O_{12}$ electrode reaction and is not corroded by HF. This result is well-matched with that of Figure 5b,c.

3.5. XPS Analysis. To verify the mechanism difference of surface layer formation between electrode with no additive and with PTSI during cycling tests, XPS was employed to investigate the element composition of $Li_4Ti_5O_{12}$ surfaces after 100 cycles at 55 °C, as given in Figure 7. It is observation that there are peaks of Ti $2p^{3/2}$ (458.6 eV) and Ti $2p^{1/2}$ (464.4 eV), which is in good conformity with Ti^{4+} ion in $Li_4Ti_5O_{12}$.[30] However, the peaks of Ti $2p_{3/2}$ and Ti $2p_{1/2}$ totally disappeared for the elelectrode with no additive. It may be ascribed that the $Li_4Ti_5O_{12}$ particle is coated with a thicker layer as reaction products of $Li_4Ti_5O_{12}$ and electrolyte decomposition. The peaks of the $Li_4Ti_5O_{12}$ electrode with 0.5 wt % PTSI were still detected. It is confirmed that PTSI

DOI: 10.1021/acsami.5b07047
ACS Appl. Mater. Interfaces 2015, 7, 23605−23614

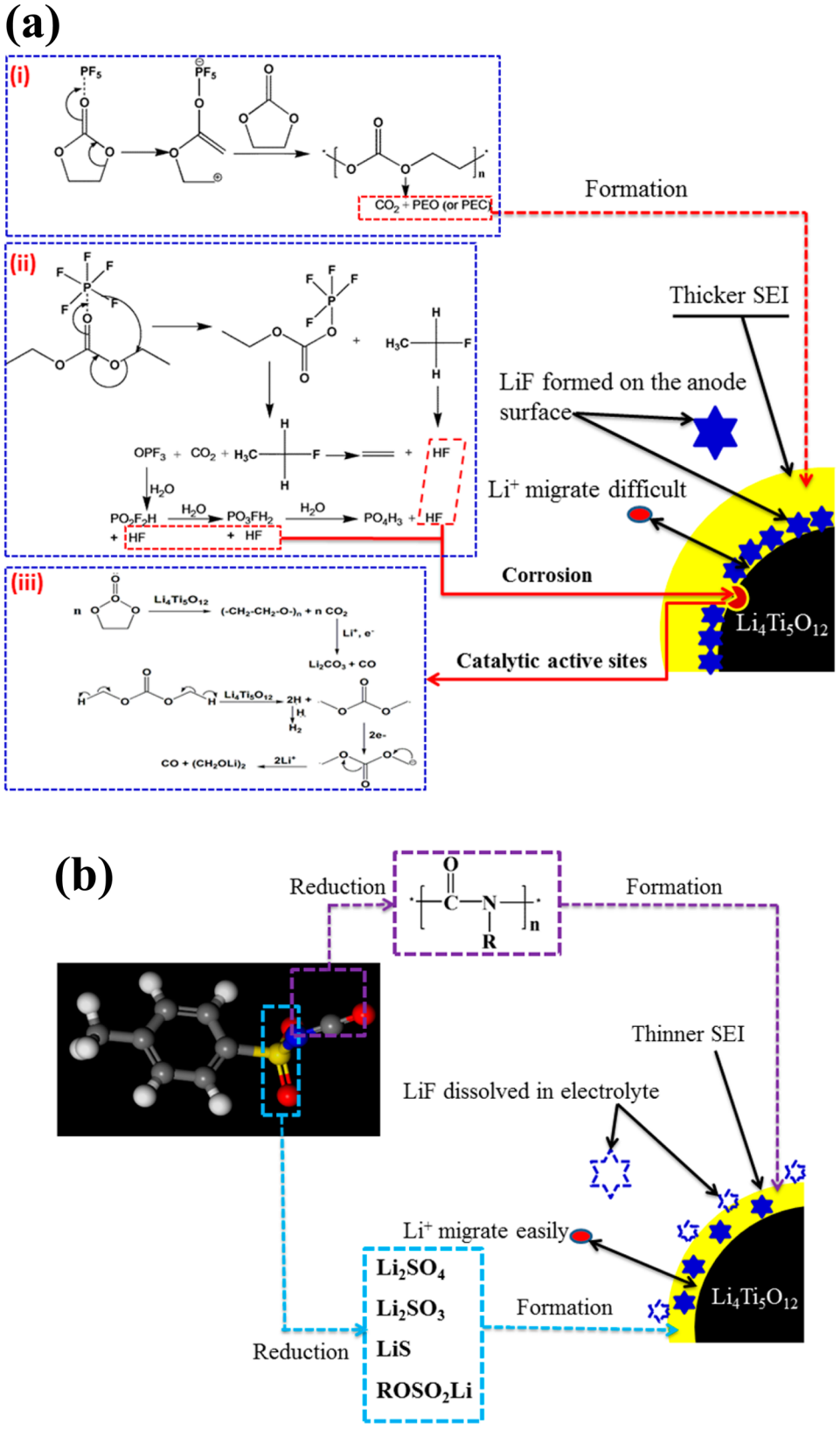

Figure 8. Schematic of mechanisms to enhance the performance of $Li_4Ti_5O_{12}$ in (a) no additive electrolyte and (b) electrolyte containing 0.5 wt % PTSI.

can suppress the decomposition of the carbonate solvents between $Li_4Ti_5O_{12}$ and electrolyte solution.

The obtained C 1s spectra indicate that the main reaction products of the SEI film are composed of species containing C−O groups. The intensities of C−C, R−CH_2OCO_2−Li, and C═O bonds observed for the electrode with 0.5 wt % PTSI are much weaker than those of the electrode with no additive. Moreover, the intensity of Li_2CO_3 for the electrode containing PTSI additive is lower than that of the electrode with no additive, suggesting that the cycled electrode is coated with less inorganic

DOI: 10.1021/acsami.5b07047
ACS Appl. Mater. Interfaces 2015, 7, 23605−23614

decomposition products. The result verifies that the SEI film on $Li_4Ti_5O_{12}$ electrode with 0.5 wt % PTSI is thinner than that of the electrode without additive.

The obtained O 1s spectra indicate that there is a major C−O peak (532.8 eV), whereas three minor peaks are, respectively, ascribed to Li_2CO_3 (531.8 eV), C═O species (532.4 eV), and the oxygen atom bonded with two carbon atoms in lithium alkyl carbonates (R−C−O−COOLi, 533.8 eV).[31,32] The relative intensity of Li_2CO_3 and C═O peaks decrease when 0.5 wt % PTSI is added into the electrolyte. It is shown that the influences of EC and DEC polymerization are obviously prevented by the addition of PTSI.

The F 1s spectra show obvious differences among the anodes cycled with two electrolytes. The peaks of LiF (684.5 eV) and $LiP_xO_yF_z$ (687.0 eV) of the $Li_4Ti_5O_{12}$ electrode with 0.5 wt % PTSI show much weaker intensity than those of the electrode with no additive, indicating that the electrode surface is covered with less inorganic produces.[33−36] The enhanced performance for the electrode with 0.5 wt % PTSI can be attributed to the $Li_4Ti_5O_{12}$ surface film with less LiF, which heightens the charge transport interface between the electrode active particles and liquid electrolyte.[37]

N 1s and S 2p spectra of the electrode with PTSI are also observed. There are N−C (399.5 eV) and N═C (401.3 eV) peaks in the N 1s spectra. Four peaks of the S 2p spectra can be detected.[38] The peaks at 167.5 and 169.8 eV belong to Li_2SO_3 and Li_2SO_4, respectively, and those at 163.3 and 168.2 eV are attributed to Li_2S and $ROSO_2Li$, respectively.[39] The result again confirms that PTSI participated in the formation of SEI film.

As discussed, SEM, XRD, TEM, and XPS data show that the formed SEI film is related to the addition of PTSI. The SEI film on the $Li_4Ti_5O_{12}$ electrode with 0.5 wt % PTSI is thinner than that of the electrode with no additive. The improvement of SEI film can inhance the transportation of Li^+ and inhibit the reaction of the electrode/electrolyte interface to a large extent.

3.6. Mechanism for Electrode/Electrolyte Interface Film. A possible mechanism of the improvement interface film between electrode and electrolyte is discussed below.

Thermal instability of $LiPF_6$-based electrolytes at elevated temperature is ascribed to the reaction as shown in Scheme 1.[40] Moreover, the decomposition reactions of EC and DEC induced by PF_5 are respectively depicted in Figure 8a (i and ii). EC ring-opening polymerization into poly(ethylene carbonate) (PEC)- or poly(ethylene oxide) (PEO)-like products is induced by PF_5.[41,42] DEC-based electrolyte attacked by PF_5 is decomposed, resulting in HF produced by side reactions (Figure 8a, ii).[20] Besides of those, even with the lack of H_2O and other acidic impurities, the stability of the SEI film worsened by PF_5 is attributed to a series of reactions with most of the SEI components, including $LiCO_3$, RCO_2Li, and $ROCO_2Li$, for example

$$Li_2CO_3 + PF_5 \rightarrow POF_3 + 2LiF + CO_2 \quad (1)$$

$$RCO_2Li + PF_5 \rightarrow RCOF + LiF + POF_3 \quad (2)$$

$$ROCO_2Li + PF_5 \rightarrow RF + LiF + CO_2 + POF_3 \quad (3)$$

The LiF content in the SEI film is augmented via these reactions. Therefore, the efforts to stabilize the electrolytes have been mainly to solve the thermal instability. For the above problem, the key is to weaken the reactivity and acidity of PF_5 via adding a little Lewis basic additive. On account of the electron-deficient PF_5, electron-rich compounds can be selected to solve the problem. PTSI includes SO_3, and the S═O groups can delocalize the nitrogen core, which acts as the weak base site to hinder the reactivity of PF_5.[21,22] Hence, HF generation and LiF formation are suppressed, resulting in formation of a thinner, modified film on the electrode and reducing interfacial resistance between the $Li_4Ti_5O_{12}$ electrode and electrolyte.

In addition, the SEI film on the $Li_4Ti_5O_{12}$ electrode with no additive is corroded by HF, resulting in the catalytic active sites of $Li_4Ti_5O_{12}$.[43] The $Li_4Ti_5O_{12}$ electrode initiates the decomposition reactions of EC and DEC,[21] resulting in poor cycling performance of cells. The possible reaction mechanism is described in Figure 8a (iii). However, PTSI participates in the formation of SEI film and successfully hinders HF erosion of the $Li_4Ti_5O_{12}$ electrode.

The serious oxidation decomposition of carbonate base electrolyte at elevated temperature can be effectively suppressed by addition of 0.5 wt % PTSI. As a result, Lewis acid is restrained, and HF formation is reduced upon heating and combustion. HF formation is effectively suppressed by decreasing the reaction of PF_5, reducing the amount of LiF in the $Li_4Ti_5O_{12}$ electrode. Hence, the performance of $Li/Li_4Ti_5O_{12}$ cell can be dramatically enhanced.

4. CONCLUSIONS

A possible mechanism of the improvement interface film between electrode and electrolyte has been presented by LSV, CV, EIS, SEM, XRD, TEM, and XPS data to understand better the roles of the additive in capacity retention upon cycling. We have proven that PTSI has a higher potential to the carbonate base electrolyte and participates in the formation of the SEI layer on the $Li_4Ti_5O_{12}$ electrode surface, which hinders the decomposition of electrolyte and depresses the interfacial reaction between electrolyte and the $Li_4Ti_5O_{12}$ electrode during cycling. The stable SEI layer originating from PTSI effectively suppresses LiF formation and obviously reduces interfacial resistance; hence, the incorporation of PTSI into the electrolyte can remarkably enhance the cyclic performance of the $Li/Li_4Ti_5O_{12}$ cell.

AUTHOR INFORMATION

Corresponding Author

*Tel./Fax: +86 731 88836633. E-mail: 703131039@qq.com, xinhaili_csu@126.com.

Notes

The authors declare no competing financial interest.

ACKNOWLEDGMENTS

This work was financially supported by the National Basic Research Program of China (973 Program, 2014CB643406).

REFERENCES

(1) Ohzuku, T.; Ueda, A.; Yamamoto, N. Zero-Strain Insertion Material of $Li[Li_{1/3}Ti_{5/3}]O_4$ for Rechargeable Lithium Cells. *J. Electrochem. Soc.* **1995**, *142*, 1431−1435.

(2) Bruce, P. G.; Scrosati, B.; Tarascon, J. M. Nanomaterials for Rechargeable Lithium Batteries. *Angew. Chem., Int. Ed.* **2008**, *47*, 2930−2946.

(3) Chen, Z. H.; Belharouak, I.; Sun, Y. K.; Amine, K. Titanium-Based Anode Materials for Safe Lithium-Ion Batteries. *Adv. Funct. Mater.* **2013**, *23*, 959−969.

(4) Young, D.; Ransil, A.; Amin, R.; Li, Z.; Chiang, Y. M. Electronic Conductivity in the $Li_{4/3}Ti_{5/3}O_4$-$Li_{7/3}Ti_{5/3}O_4$ System and Variation with

DOI: 10.1021/acsami.5b07047
ACS Appl. Mater. Interfaces 2015, 7, 23605−23614

State-of-Charge as a Li Battery Anode. *Adv. Energy Mater.* **2013**, *3*, 1125−1129.
(5) Yu, S. H.; Pucci, A.; Herntrich, T.; Willinger, M. G.; Baek, S. H.; Sung, Y. E.; Pinna, N. Surfactant-Free Nonaqueous Synthesis of Lithium Titanium Oxide (LTO) Nanostructures for Lithium Ion Battery Applications. *J. Mater. Chem.* **2011**, *21*, 806−810.
(6) Wang, Y. G.; Liu, H. K.; Wang, K. X.; Eiji, H.; Wang, Y. K.; Zhou, H. S. Synthesis and Electrochemical Performance of Nano-sized $Li_4Ti_5O_{12}$ with Double Surface Modification of Ti(III) and Carbon. *J. Mater. Chem.* **2009**, *19*, 6789−6795.
(7) Shen, L. F.; Yuan, C. Z.; Luo, H. J.; Zhang, X. G.; Xu, K.; Zhang, F. In Situ Growth of $Li_4Ti_5O_{12}$ on Multi-Walled Carbon Nanotubes: Novel Coaxial Nanocables for High Rate Lithium Ion Batteries. *J. Mater. Chem.* **2011**, *21*, 761−767.
(8) Cheng, L.; Yan, J.; Zhu, G. N.; Luo, J. Y.; Wang, C. X.; Xia, Y. Y. General Synthesis of Carbon-Coated Nanostructure $Li_4Ti_5O_{12}$ as a High Rate Electrode Material for Li-ion Intercalation. *J. Mater. Chem.* **2010**, *20*, 595−602.
(9) Aldon, L.; Kubiak, P.; Womes, M.; Jumas, J. C.; Olivier-Fourcade, J.; Tirado, J. L.; Corredor, J. I.; Pérez Vicente, C. Chemical and Electrochemical Li-Insertion into the $Li_4Ti_5O_{12}$ Spinel. *Chem. Mater.* **2004**, *16*, 5721−5725.
(10) Li, B.; Han, C.; He, Y. B.; Yang, C.; Du, H.; Yang, Q. H.; Kang, F. Facile Synthesis of $Li_4Ti_5O_{12}$/C Composite with Super Rate Performance. *Energy Environ. Sci.* **2012**, *5*, 9595−9602.
(11) Wang, Y. Q.; Gu, L.; Guo, Y. G.; Li, H.; He, X. Q.; Tsukimoto, S.; Ikuhara, Y.; Wan, L. J. Rutile-TiO_2 Nanocoating for a High-Rate $Li_4Ti_5O_{12}$ Anode of a Lithium-Ion Battery. *J. Am. Chem. Soc.* **2012**, *134*, 7874−7879.
(12) He, Y. B.; Li, B.; Liu, M.; Zhang, C.; Lv, W.; Yang, C.; Li, J.; Du, H.; Zhang, B.; Yang, Q. H.; Kim, J. K.; Kang, F. Gassing in $Li_4Ti_5O_{12}$-Based Batteries and its Remedy. *Sci. Rep.* **2012**, *2*, 913−921.
(13) Wang, R. H.; Li, X. H.; Zhang, B.; Wang, Z. X.; Guo, H. J. Effect of Methylene Methanedisulfonate as an Additive on the Cycling Performance of Spinel Lithium Titanate Electrode. *J. Alloys Compd.* **2015**, *648*, 512−520.
(14) Zhao, L.; Hu, Y. S.; Li, H.; Wang, Z. X.; Chen, L. Q. Porous $Li_4Ti_5O_{12}$ Coated with N-Doped Carbon from Ionic Liquids for Li-Ion Batteries. *Adv. Mater.* **2011**, *23*, 1385−1388.
(15) Kim, J. G.; Shi, D. Q.; Park, M. S.; Jeong, G.; Heo, Y. U.; Seo, M.; Kim, Y. J.; Kim, J. H.; Dou, S. X. Controlled Ag-Driven Superior Rate-Capability of $Li_4Ti_5O_{12}$ Anodes for Lithium Rechargeable Batteries. *Nano Res.* **2013**, *6*, 365−372.
(16) Zhang, Y. Y.; Zhang, C. M.; Lin, Y.; Xiong, D. B.; Wang, D.; Wu, X. Y.; He, D. N. Influence of Sc^{3+} Doping in B-Site on Electrochemical Performance of $Li_4Ti_5O_{12}$ Anode Materials for Lithium-Ion Battery. *J. Power Sources* **2014**, *250*, 50−57.
(17) Zhang, B.; Liu, Y. S.; Huang, Z. D.; Oh, S.; Yu, Y.; Mai, Y.-W.; Kim, J. K. Urchin-Like $Li_4Ti_5O_{12}$−Carbon Nanofiber Composites for High Rate Performance Anodes in Li-Ion Batteries. *J. Mater. Chem.* **2012**, *22*, 12133−12140.
(18) Zhang, B.; Yu, Y.; Liu, Y.; Huang, Z. D.; He, Y. B.; Kim, J. K. Percolation Threshold of Graphene Nanosheets as Conductive Additive in $Li_4Ti_5O_{12}$ Anodes of Li-ion Batteries. *Nanoscale* **2013**, *5*, 2100−2107.
(19) Zhang, S. S. A Review on Electrolyte Additives for Lithium-Ion Batteries. *J. Power Sources* **2006**, *162*, 1379−94.
(20) He, Y. B.; Liu, M.; Huang, Z. D.; Zhang, B.; Yu, Y.; Li, B. H.; Kang, F. Y.; Kim, J. K. Effect of Solid Electrolyte Interface (SEI) Flm on Cyclic Performance of $Li_4Ti_5O_{12}$ Anodes for Li Ion Batteries. *J. Power Sources* **2013**, *239*, 269−276.
(21) Wu, F.; Xiang, J.; Li, L.; Chen, J. Z.; Tan, G. Q.; Chen, R. J. Study of the Electrochemical Characteristics of Sulfonyl Isocyanate/Sulfone Binary Electrolytes for Use in Lithium-Ion Batteries. *J. Power Sources* **2012**, *202*, 322−331.
(22) Xu, K. Nonaqueous Liquid Electrolytes for Lithium-Based Rechargeable Batteries. *Chem. Rev.* **2004**, *104*, 4303−4417.
(23) Funabiki, A.; Inaba, M.; Ogumi, Z. A.c. Impedance Analysis of Electrochemical Lithium Intercalation into Highly Oriented Pyrolytic Graphite. *J. Power Sources* **1997**, *68*, 227−231.
(24) Aurbach, D.; Levi, M. D.; Levi, E. Common Electroanalytical Behavior of Li Intercalation Processes into Graphite and Transition Metal Oxides. *J. Electrochem. Soc.* **1998**, *145*, 3024−3034.
(25) Levi, M. D.; Gamolsky, K.; Aurbach, D.; Heider, U.; Oesten, R. On Electrochemical Impedance Measurements of $Li_xCo_{0.2}Ni_{0.8}O_2$ and Li_xNiO_2 Intercalation Electrodes. *Electrochim. Acta* **2000**, *45*, 1781−1789.
(26) Feng, J.; Huang, Z.; Guo, C.; Chernova, N. A.; Upreti, S.; Whittingham, M. S. An Organic Coprecipitation Route to Synthesize High Voltage $LiNi_{0.5}Mn_{1.5}O_4$. *ACS Appl. Mater. Interfaces* **2013**, *5*, 10227−10232.
(27) Dedryvere, R.; Foix, D.; Franger, S.; Patoux, S.; Daniel, L.; Gonbeau, D. Electrode/Electrolyte Interface Reactivity in High-Voltage Spinel $LiMn_{1.6}Ni_{0.4}O_4/Li_4Ti_5O_{12}$ Lithium-Ion Battery. *J. Phys. Chem. C* **2010**, *114*, 10999−11008.
(28) Park, G.; Nakamura, H.; Lee, Y.; Yoshio, M. The Important Role of Additives for Improved Lithium Ion Battery Safety. *J. Power Sources* **2009**, *189*, 602−606.
(29) Jiang, C. H.; Zhou, Y.; Honma, I.; Kudo, T.; Zhou, H. S. Preparation and Rate Capability of $Li_4Ti_5O_{12}$ Hollow-Sphere Anode Material. *J. Power Sources* **2007**, *166*, 514−518.
(30) Li, Y.; Pan, G. L.; Liu, J. W.; Gao, X. P. Preparation of $Li_4Ti_5O_{12}$ Nanorods as Anode Materials for Lithium-Ion Batteries. *J. Electrochem. Soc.* **2009**, *156*, A495−A499.
(31) Herstedt, M.; Andersson, A. M.; Rensmo, H.; Siegbahn, H.; Edstrom, K. Characterisation of the SEI Formed on Natural Graphite in PC-Based Electrolytes. *Electrochim. Acta* **2004**, *49*, 4939−4947.
(32) Dedryvere, R.; Gireaud, L.; Grugeon, S.; Laruelle, S.; Tarascon, J. M.; Gonbeau, D. Characterization of Lithium Alkyl Carbonates by X-ray Photoelectron Spectroscopy: Experimental and Theoretical Study. *J. Phys. Chem. B* **2005**, *109*, 15868−15875.
(33) Ryou, M. H.; Han, G. B.; Lee, Y. M.; Lee, J. N.; Lee, D. J.; Yoon, Y. O.; Park, J. K. Effect of Fuoroethylene Carbonate on High Temperature Capacity Retention of $LiMn_2O_4$/Graphite Li-Ion Cells. *Electrochim. Acta* **2010**, *55*, 2073−2077.
(34) Zhou, L.; Dalavi, S.; Xu, M. Q.; Lucht, B. Effects of Different Electrode Materials on the Performance of Lithium Tetrafluorooxalatophosphate (LiFOP) Electrolyte. *J. Power Sources* **2011**, *196*, 8073−8084.
(35) Xu, M. Q.; Hao, L. S.; Liu, Y. L.; Li, W. S.; Xing, L. D.; Li, B. Experimental and Theoretical Investigations of Dimethylacetamide (DMAc) as Electrolyte Stabilizing Additive for Lithium Ion Batteries. *J. Phys. Chem. C* **2011**, *115*, 6085−6094.
(36) Park, J. H.; Kim, J. S.; Shim, E. G.; Park, K. W.; Hong, Y. T.; Lee, Y. S.; Lee, S. Y. Polyimide Gel Polymer Electrolyte-Nanoencapsulated $LiCoO_2$ Cathode Materials for High-Voltage Li-Ion Batteries. *Electrochem. Commun.* **2010**, *12*, 1099−1102.
(37) Petibon, R.; Henry, E. C.; Burns, J. C.; Sinha, N. N.; Dahn, J. R. Comparative Study of Vinyl Ethylene Carbonate (VEC) and Vinylene Carbonate (VC) in $LiCoO_2$/Graphite Pouch Cells Using High Precision Coulometry and Electrochemical Impedance Spectroscopy Measurements on Symmetric Cells. *J. Electrochem. Soc.* **2014**, *161*, A66−A74.
(38) Wang, B.; Qu, Q. T.; Yang, L. C.; Xia, Q.; Wu, Y. P.; Zhou, D. L.; Gu, X. J.; van Ree, T. 2-Phenylimidazole as an Additive to Prevent the Co-Intercalation of Propylene Carbonate in Organic Electrolyte for Lithium-Ion Batteries. *J. Power Sources* **2009**, *189*, 757−760.
(39) Li, B.; Xu, M. Q.; Li, B. Z.; Liu, Y.; Yang, L.; Li, W.; Hu, S. J. Properties of Solid Electrolyte Interphase Formed by Prop-1-Ene-1,3-Sultone on Graphite Anode of Li-Ion Batteries. *Electrochim. Acta* **2013**, *105*, 1−6.
(40) Xu, G. J.; Liu, Z. H.; Zhang, C. J.; Cui, G. L.; Chen, L. Q. Strategies for Improving the Cyclability and Thermo-Stability of $LiMn_2O_4$-Based Batteries at Elevated Temperatures. *J. Mater. Chem. A* **2015**, *3*, 4092−4123.
(41) Sloop, S. E.; Kerr, J. B.; Kinoshita, K. The Role of Li-Ion Battery Electrolyte Reactivity in Performance Decline and Self-Discharge. *J. Power Sources* **2003**, *119−121*, 330−337.

DOI: 10.1021/acsami.5b07047
ACS Appl. Mater. Interfaces 2015, 7, 23605−23614

(42) Andersson, A. M.; Edstrom, K. Chemical Composition and Morphology of the Elevated Temperature SEI on Graphite. *J. Electrochem. Soc.* **2001**, *148*, A1100−A1109.
(43) He, Y.; Ning, F.; Li, B.; Song, Q.; Lv, W.; Du, H.; Zhai, D.; Su, F.; Yang, Q.; Kang, F. Carbon Coating to Suppress the Reduction Decomposition of Electrolyte on the $Li_4Ti_5O_{12}$ Electrode. *J. Power Sources* **2012**, *202*, 253−261.

DOI: 10.1021/acsami.5b07047
ACS Appl. Mater. Interfaces 2015, 7, 23605−23614